JOURNAL OF APPLIED ELECTROCHEMISTRY 25 (1995) 565–573

Modelling of time-dependent performance criteria in a three-dimensional cell system during batch recirculation copper recovery

V. D. STANKOVIC

Technical Faculty Bor, University of Belgrade, JNA12, 19210 Bor, Yugoslavia

A. A. WRAGG

School of Engineering, University of Exeter, Exeter EX4 4QF, Great Britain

Received 18 May 1994; revised 5 December 1994

A three-dimensional electrode cell with cross-flow of current and electrolyte is modelled for galvanostatic and pseudopotentiostatic operation. The model is based on the electrodeposition of copper from acidified copper sulphate solution onto copper particles, with an initial concentration ensuring a diffusion-controlled process and operating in a batch recycle mode. Plug flow through the cell and perfect mixing of the electrolyte in the reservoir are assumed. Based on the model, the behaviour of reacting ion concentration, current efficiency, cell voltage, specific energy consumption and process time on selected independent variables is analysed for both galvanostatic and pseudopotentiostatic modes of operation. From the results presented it is possible to identify the optimal values of parameters for copper electrowinning.

List of symbols

a	specific surface area (m^{-1})
A	cross-sectional area (m^2)
a_a	Tafel constant for anode overpotential (V)
a_H	Tafel constant for hydrogen evolution overpotential (V)
b_a	Tafel coefficient for anode overpotential ($V\,decade^{-1}$)
b_H	Tafel coefficient for hydrogen evolution overpotential ($V\,decade^{-1}$)
C_e	concentration at the electrode surface (M)
C_L	cell outlet concentration (M)
C_0	cell inlet concentration (M)
C_0^0	initial cell inlet concentration at $t = 0$ (M)
d_p	particle diameter (m)
e, e_p	current efficiency and pump efficiency, respectively
E	specific energy consumption ($Wh\,mol^{-1}$)
ΔE	solution phase potential drop through the cathode (V)
F	Faraday number ($C\,mol^{-1}$)
Δh	interelectrode distance (m)
i, i_L	current density and limiting current density, respectively ($A\,m^{-2}$)
I, I_L	current and limiting current, respectively (A)
I_H	partial current for hydrogen evolution (A)
k_L	mass transfer coefficient ($m\,s^{-1}$)
L	bed height (m)
Δl	bed depth (m)
M	molecular weight ($g\,mol^{-1}$)
N	power per unit of electrode area ($W\,m^{-2}$)
n	exponent in Equation 19
ΔP	pressure drop in the cell ($N\,m^{-2}$)
Q	electrolyte flow rate ($m^3\,h^{-1}$)
R	Universal gas constant ($J\,mol^{-1}\,K^{-1}$)
r_e	electrochemical reaction rate ($mol\,m^{-2}\,h^{-1}$)
t_c	critical time for operating current to reach instantaneous limiting current (s)
t_p	process time to reach specified degree of conversion (s)
T	temperature (K)
u	electrolyte velocity ($m\,s^{-1}$)
U	total cell voltage (V)
U_0	reversible decomposition potential (V)
ΔU_{ohm}	ohmic voltage drop between anode and three-dimensional cathode (V)
V	volume of electrolyte (m^3)
z	number of transferred electrons

Greek letters

α	ratio of the operating and limiting currents
$\eta_{A,a}$	anodic activation overpotential (V)
$\eta_{C,c}$	cathodic concentration overpotential (V)
ϵ	bed voidage
ϵ_H	void fraction of hydrogen bubbles in cathode
γ	constant (Equation 2)
κ_0	electrolyte conductivity ($ohm^{-1}\,m^{-1}$)
ν	electrolyte kinematic viscosity ($m^2\,s^{-1}$)
$\Delta\phi_d$	diaphragm voltage drop (V)
$\Delta\phi_H$	voltage drop due to hydrogen bubble containing electrolyte in cathode (V)
ρ	electrolyte density ($kg\,m^{-3}$)
ρ_p	particle density ($kg\,m^{-3}$)
τ	reservoir residence time (s)

0021-891X

1. Introduction

There has recently been considerable research interest in the performance of three-dimensional electrodes such as fixed- and fluidized beds of conductive particles [1–6], and other variant cells of these types such as the spouted bed [7–9], the vortex bed [10] and the circulating bed [11]. Features such as high electrode specific surface area and good mixing and mass transfer rates suggest that three-dimensional electrodes possess significant advantages over conventional plate cells in a variety of areas like electro-organic synthesis [12, 13] and metal recovery and removal from waste streams [4–6, 14–16], and leach liquors [2, 5, 8]. A particularly interesting area for the application of three-dimensional electrodes is the periodic treatment of small volumes of rinse waters from galvanizing plants, copper and brass rolling plants and the electronics industry.

One possible mode of operation of a three-dimensional electrode cell involves continuous recirculation of electrolyte so that a gradual depletion of the concentration of metal ions takes place. In the design of such a process, the prediction of the change of concentration of the reacting ions with time is important. Furthermore, during removal of metal ions, not only does concentration vary with time, but also the limiting current, the current efficiency, the cell voltage and the energy consumption, as well as other parameters which characterise the overall performance of the reactor system. The objective of the present work is to analyse the behaviour with time of the significant performance parameters mentioned above for a three-dimensional fluidized bed cell operated in batch recirculating mode using a simple theoretical model. The analysis has been made for the commonly used galvanostatic mode of operation and for the case of decrease of operating current with time, a pseudo-potentiostatic mode.

2. Model formulation

2.1. *Basic assumptions*

A one dimensional model similar to that derived for the fixed bed electrode [17] and the fluidized bed electrode [18, 19] is based on the following assumptions:

(i) As a model electrode reaction the electrodeposition of copper from acidified copper sulphate solution is used. The initial concentration of Cu^{2+} ions is such as to ensure a diffusion controlled process.

(ii) The anode reaction is oxygen evolution.

(iii) The feeder electrode and anode are flat plates situated in a side by side configuration. Spherical monosized copper particles in contact with the copper feeder form the three-dimensional electrode.

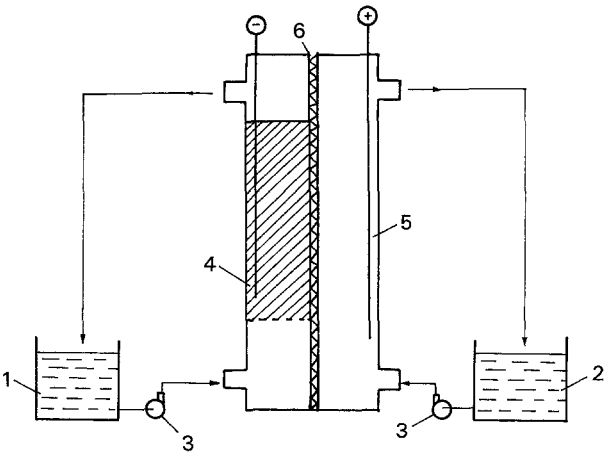

Fig. 1. Schematic view of the batch recirculation electrochemical system. (1) Catholyte reservoir, (2) anolyte reservoir, (3) pumps, (4) cathode feeder, (5) anode and (6) separator.

(iv) The anode and cathode spaces are separated by a diaphragm, the resistance of which is assumed to be constant during the process.

(v) The current flow is normal to that of the electrolyte.

(vi) Plug flow occurs in the cathode compartment and there is perfect mixing in the reservoir.

(vii) The Cu^{2+} ion depletion process occurs under constant geometric and hydrodynamic conditions.

(viii) Constant physical properties of the electrolyte are assumed.

(xi) A sufficient quantity of supporting electrolyte is assumed to be present in the electrolyte to render Cu^{2+} ion migration negligible.

(x) The mass transfer coefficient is constant both temporally and spacially.

A schematic view of the cell and circulation system is shown in Fig. 1 and data used in the model computation are listed in Table 1.

2.2. *Concentration–time relationship for limiting current conditions*

The change in concentration as a function of time for a plug flow reactor coupled to a well mixed reservoir for a diffusion controlled process is given by [18]

$$C_0(t) = C_0^0 \exp\left\{-\frac{tQ}{V}\left[1 - \exp\left(-\frac{k_L a L}{u}\right)\right]\right\} \quad (1)$$

Table 1. Value of parameters used in calculations [17]

$z = 2$	$k_L = 7.7 \times 10^{-5}\,\mathrm{m\,s^{-1}}$
$F = 96500\,\mathrm{C\,mol^{-1}}$	$\rho_p = 8800\,\mathrm{kg\,m^{-3}}$
$C_0^0 = 1\,\mathrm{g\,dm^{-3}}$	$\nu = 1.037 \times 10^{-6}\,\mathrm{m^2\,s^{-1}}$
$h = 0.01\,\mathrm{m}$	$D = 5.57 \times 10^{-10}\,\mathrm{m^2\,s^{-1}}$
$L = 1\,\mathrm{m}$	$\kappa_0 = 50\,\Omega^{-1}\,\mathrm{m^{-1}}$
$B = 1\,\mathrm{m}$	$T = 298\,\mathrm{K}$
$\epsilon_0 = 0.42$	$\rho = 1070\,\mathrm{kg\,m^{-3}}$
$U_0 = 0.828\,\mathrm{V}$	$a_H = 0.24\,\mathrm{V}$
$a_a = 0.5\,\mathrm{V}$	$b_H = 0.12\,\mathrm{V}$
$b_a = 0.12\,\mathrm{V}$	$V = 1\,\mathrm{m^3}$
$d_p = 1\,\mathrm{mm}$	$\Delta\phi_d = 0.1\,\mathrm{V}$
$u = 0.06\,\mathrm{m\,s^{-1}}$	$R = 8.314\,\mathrm{J\,mol^{-1}\,K^{-1}}$

Putting $V/Q = \tau$ as the mean reservoir residence time, and assuming constant hydrodynamic conditions, Equation 1 may be reduced to

$$C_0(t) = C_0^0 \exp\left(-\frac{t\gamma}{\tau}\right) \tag{2}$$

where

$$\gamma = 1 - \exp\left(\frac{k_L a L}{u}\right)$$

These equations are obtained assuming that the cell works under limiting current conditions at all times and thus correspond to the maximum degree of conversion.

3. Galvanostatic operation

3.1. *Change of limiting current with time*

For the case of galvanostatic operation (I = const.), when the operating current is less than the initial limiting current

$$I = \alpha I_L(0) \tag{3}$$

where $0 < \alpha < 1$, the depletion process involves two periods [9, 17] relative to the limiting current. The limiting current as a function of distance and time may be expressed in the following form [18, 19]:

$$dI_L(y, t) = zFk_L aAC(y, t)\,dy \tag{4}$$

Integrating Equation 4 over the electrode length gives

$$I_L(t) = zFuAC_0(t) \tag{5}$$

indicating similar behaviour of limiting current and concentration with time.

Both Equations 1 and 5 are approximate solutions of the given differential equation. Walker and Wragg [18] have published more exact solutions and have also shown that an approximate solution is sufficiently accurate for many practical purposes.

For the first period of the depletion process, when the operating current is less than the limiting current (i.e., $I < I_L(t)$) cell productivity is less than the maximum productivity as defined by Equation 1. In this period the current efficiency is high and the concentration of reacting ions changes linearly with time according to Faraday's law. For the second period, when the value of operating current exceeds the value of the instantaneous limiting current (i.e., $I > I_L(t)$) simultaneous hydrogen evolution occurs. For this period, the operating current may be expressed as a sum of the instantaneous limiting current and the hydrogen production partial current [10, 17]:

$$I = I_L(t) + I_H(t) \tag{6}$$

As a consequence of hydrogen evolution the current efficiency decreases with time. The onset of hydrogen evolution also produces an inevitable increase in the cell voltage and additional bubble ohmic effects are incurred [20, 21]. In this period the concentration of reacting ions decreases according to Equation 1. Similarly, the limiting current changes in accordance with Equation 5. The behaviour of the limiting current with time is shown schematically in Fig. 2. The time for the limiting current to reach the operating current is termed the critical time, t_c.

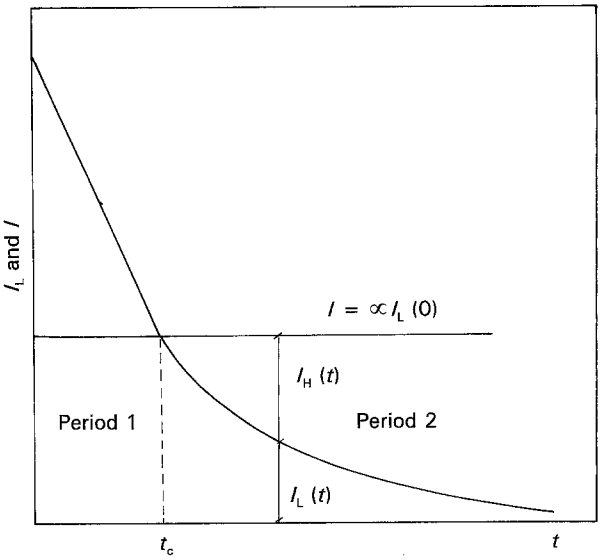

Fig. 2. Schematic presentation of limiting current behaviour with time.

3.2. *Depletion of reacting ions with time*

The change in the concentration of reacting ions for the first period of the electrowinning process, for $I < I_L(t)$, may be expressed through the cell mass balance by

$$C_0 - C_L = \frac{\alpha I_L(0)}{zFQ} \tag{7}$$

Taking into account the reservoir mass balance along with Equation 5, the following equation describing the linear change of concentration with time is obtained:

$$C_0(t) = C_0^0\left(1 - \frac{\alpha t\gamma}{\tau}\right) \tag{8}$$

The linear fall in concentration with time applies up to the critical time, t_c, at which the actual reservoir concentration is

$$C_0(t_c) = \alpha C_0^0 \tag{9}$$

Substituting Equation 9 into Equation 8 and solving for t_c gives

$$t_c = \frac{\tau(1-\alpha)}{\alpha\gamma} \tag{10}$$

When $t > t_c$, the change in concentration with time may be described by the following equation which is similar to Equation 1:

$$C_0(t) = \alpha C_0^0 \exp\left(-\frac{t\gamma}{\tau} + \frac{1-\alpha}{\alpha}\right) \tag{11}$$

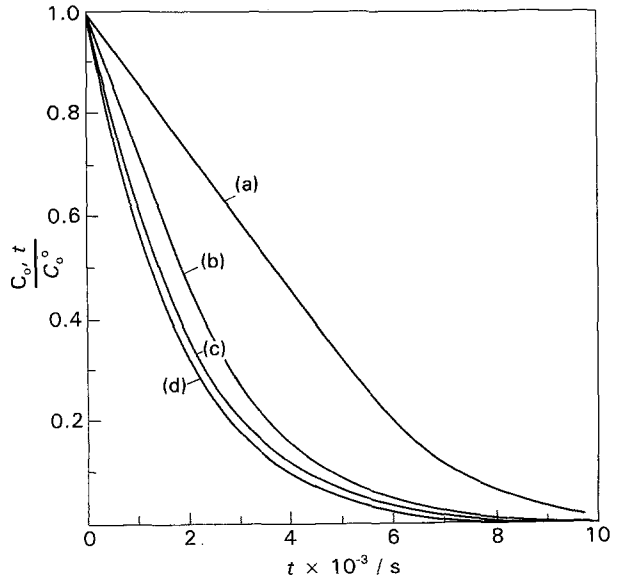

Fig. 3. Variation of concentration of reacting ions with time (galvanostatic conditions) at various values of α: (a) $\alpha = 0.25$, (b) $\alpha = 0.5$, (c) $\alpha = 0.75$ and (d) $\alpha = 1.0$.

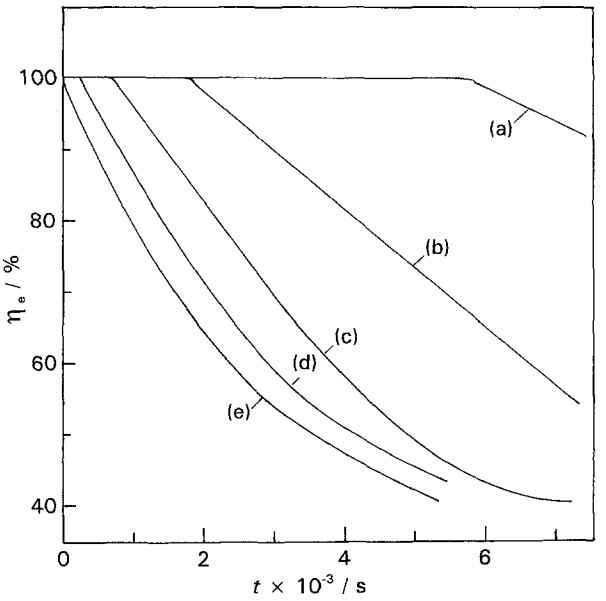

Fig. 4. Current efficiency against time at different α for galvanostatic conditions: (a) $\alpha = 0.25$, (b) $\alpha = 0.5$, (c) $\alpha = 0.75$, (d) $\alpha = 0.9$ and (e) $\alpha = 1.0$.

Examples of the decrease in concentration with time for both the first and second periods is presented in Fig. 3, for different values of the parameter α.

It is clear that with increasing α, the linear portion of the curve becomes shorter so that for $\alpha = 1$ it has the form described by Equation 1. It may also be seen in Fig. 3 that with increasing α, the curves become closer, finally approaching the maximum rate of conversion obtained for an operating current equal to the initial limiting current (i.e., $I = I_L(0)$).

3.3. *Current efficiency*

The current efficiency for copper deposition may be expressed as:

$$e = \frac{zFV[C_0^0 - C_0(t)]}{It} \tag{12}$$

For the first period of the process, when $I < I_L(t)$, substituting Equation 8 into Equation 12, and introducing:

$$I = \alpha z F u A \gamma C_0^0 \tag{13}$$

as the expression for $I = I_L(0)$ the current efficiency is found to be

$$e = 1 \quad \text{for} \quad 0 < t \leqslant t_c \tag{14}$$

Thus, the total charge passed produces the desired product. In real cells values for current efficiency may be more or less close to this theoretical value [2, 5, 9] under appropriate operating conditions. This is despite some product loss as a consequence of chemical dissolution of deposited metal due to the presence of dissolved oxygen in the electrolyte. The existence of anodic zones in the cathode space may also induce dissolution of metal, thus decreasing current efficiency [5, 8].

For the second period, when the operating current is higher than the instantaneous limiting current, substituting Equations 11 and 5 for $t = 0$ into Equation 12, the following equation is obtained:

$$e = \frac{1 - \alpha \exp[-t\gamma/\tau + (1-\alpha)/\alpha]}{\alpha t\gamma/\tau} \tag{15}$$

In Fig. 4 the change of current efficiency with time is depicted over the whole process time. Clearly higher efficiencies are obtained for longer periods with lower operating currents but process times are longer. Also, at lower operating currents the electrodeposition takes place closer to the equilibrium potential and chemical dissolution may take place thus, in practical situations, decreasing the current efficiency.

Several investigators have plotted current efficiency against the concentration of reacting ions [2, 7, 10, 22] for similar systems. Starting from this point, and with the aim of highlighting the consequences of Equation 15, Equations 8 and 11 may be solved for t and the result substituted in Equation 12. Introducing Equation 13 for the first period yields an expression identical with Equation 14. For the second period the following equation is obtained:

$$e = \frac{(1 - C_0(t)/C_0^0)}{(1-\alpha)/\alpha - \ln C_0(t)/C_0^0} \tag{16}$$

which express current efficiency in terms of concentration. Calculated values for current efficiency against concentration are presented in Fig. 5.

3.4. *Cell voltage*

The overall cell voltage may be calculated as a sum of the reversible decomposition potential, the ohmic voltage drop between the three dimensional cathode and the counter electrode, the solution potential

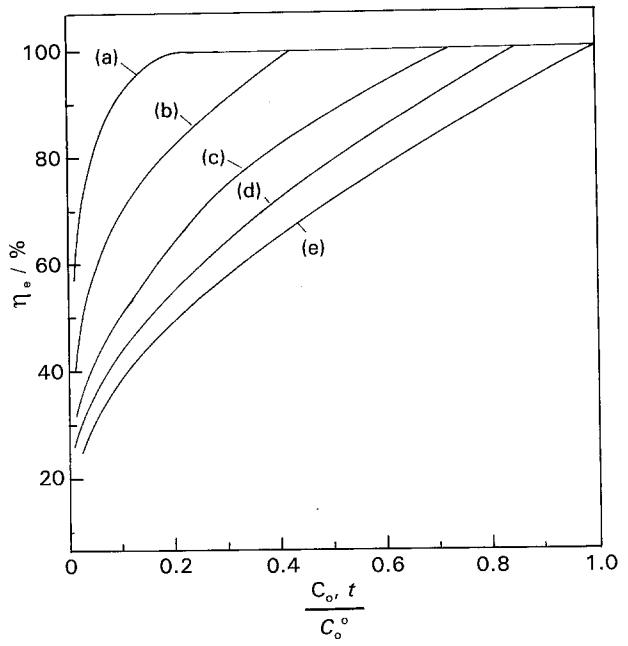

Fig. 5. Current efficiency against dimensionless concentration for galvanostatic conditions: (a) $\alpha = 0.25$, (b) $\alpha = 0.5$, (c) $\alpha = 0.75$, (d) $\alpha = 0.9$ and (e) $\alpha = 1.0$.

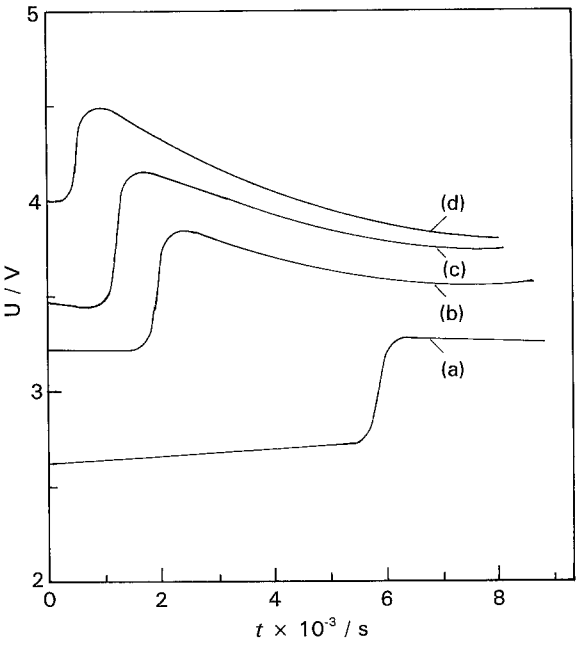

Fig. 6. Cell voltage against time for galvanostatic conditions at various values of α: (a) $\alpha = 0.25$, (b) $\alpha = 0.5$, (c) $\alpha = 0.75$ and (d) $\alpha = 1.0$.

drop through the cathode, the overpotentials and the voltage drop through the diaphragm. Thus,

$$U = U_0 + \Delta U_{\text{ohm}} + \Delta E + \eta_{A,a} + \eta_{C,c} + \Delta\phi_d \quad (17)$$

For the first period of the process when $I < I_L(t)$, Equation 17 may be written in a form in which the terms are fully defined:

$$U = U_0 + \frac{i\Delta h}{\kappa_0} + \Delta E + a_a + b_a \ln i + \frac{RT}{zF} \ln \frac{C_e}{C_b} + \Delta\phi_d \quad (18)$$

The solution potential drop through the cathode may be written as [17]

$$\Delta E = \frac{zFu^2 C_0(t)}{k_L a \kappa_0 \epsilon^n} \left[1 - \exp\left(-\frac{k_L a \Delta l}{u}\right) - \frac{k_L a \Delta l}{u}\right] \quad (19)$$

In Equation 19 the resistance of the metallic phase is omitted due to its negligibly small value.

For the second period $I \geqslant I_L(t)$, hydrogen evolution takes place, and Equation 18 has to be extended by two further terms, the hydrogen evolution activation potential, $\eta_{H,a}$ and the additional voltage drop caused by the presence of bubbles evolved in the cathode compartment. This last term is difficult to calculate since the prediction of the hydrogen bubble volume fraction, ϵ_H, is problematic (but see Appendix). For a Tafelian hydrogen overpotential, Equation 18 may be written as follows:

$$U = U_0 + \frac{i\Delta h}{\kappa_0} + \Delta E + a_a + b_a \ln i + a_H + b_H \ln i_H + \Delta\phi_H + \Delta\phi_d \quad (20)$$

The penultimate term represents the voltage drop due to hydrogen bubbles; the term is neglected in the following calculations. Using Equations 18 and 20, a family of curves was derived and is presented in Fig. 6 for different values of α, showing the behaviour of the cell voltage with time. The two periods of the process, as already discussed, are clearly recognisable in Fig. 6. When the operating current reaches the value of the instantaneous limiting current for given value of α, the cell voltage increases sharply due to the increase in concentration overpotential and the onset of hydrogen evolution, after which the cell voltage decreases slowly as shown in Fig. 6. It should be emphasized that the time to reach the sharp voltage step becomes shorter with increasing α, approaching a zero value for $\alpha = 1$, that is, for operating current equal to the initial limiting current $I_L(0)$.

Similar experimental behaviour of cell voltage with time has been confirmed [2, 9] for the electrodeposition of copper in three dimensional electrode cells.

4. Decrease of operating current with time: pseudopotentiostatic conditions

4.1. *Current–time behaviour*

If the operating current changes with time following the limiting current, that is,

$$I(t) = \alpha I_L(t) \quad (21)$$

it is possible to carry out an electrowinning process avoiding the hydrogen evolution reaction. This involves the feeder being kept at constant potential. For a diffusion controlled reaction the following relationship may be written as

$$\eta_{C,c} = \frac{RT}{zF} \ln\left(1 - \frac{I}{I_L}\right) \quad (22)$$

Substituting Equation 21 into Equation 22 gives

$$\eta_{C,c} = \frac{RT}{zF}\ln(1-\alpha) \tag{23}$$

Under these conditions the operating current must be reduced with time; from Equation 4 there follows:

$$I(t) = \alpha zFuA\gamma C_0(t) \tag{24}$$

It must be noted that the potential of a three-dimensional electrode has a complex distribution [1, 5, 13] so that the whole electrode is not at a single potential. The present model does not take into account the potential distribution either across or along the electrode. For these reasons the term pseudopotentiostatic is used here.

4.2. *Concentration–time behaviour*

The change in the concentration of reacting ions, for potentiostatic conditions, may be derived as follows. For a single pass of electrolyte through the cell, the mass balance may be written as

$$C_0 - C_L(t) = \frac{\alpha I(t)}{zFQ} \tag{25}$$

or, substituting Equation 24 into Equation 25

$$C_0 - C_L(t) = \alpha C_0(t)\gamma \tag{26}$$

Since the left hand side of Equation 26 may be substituted by the term [18, 19] $-V\mathrm{d}C_0(t)/Q\mathrm{d}t$, the following differential equation is obtained:

$$-\frac{\mathrm{d}C_0(t)}{\mathrm{d}t} = \frac{\alpha Q}{V}C_0(t)\gamma \tag{27}$$

Integrating Equation 27 for the following boundary conditions:

$$t = 0; C_0(t) = C_0, t = t; C_0(t)C_0(t)$$

gives

$$C_0(t) = C_0^0 \exp\left(-\frac{\alpha t\gamma}{\tau}\right) \tag{28}$$

In Fig. 7 the change of concentration with time is presented for different values of α, that is, for different values of cathode feeder potential.

4.3. *Current efficiency relationship*

Based on Equation 12, the equation for current efficiency may be written as

$$e = \frac{[C_0^0 - C_0(t)]zFV}{\alpha\int_0^t I_L(t)\,\mathrm{d}t} \tag{29}$$

Substituting Equation 24 into Equation 29 and integrating for a given process time gives a result identical to Equation 15. In other words, in the case of potentiostatic operation of the three-dimensional electrode, the whole charge passing through the cell produces electrodeposited copper.

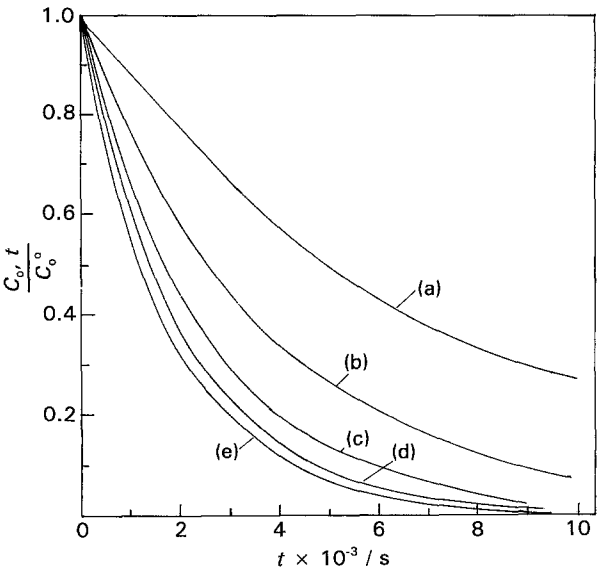

Fig. 7. Concentration–time relationship for pseudo potentiostatic mode of operation at various values of α: (a) $\alpha = 0.25$, (b) $\alpha = 0.5$, (c) $\alpha = 0.75$, (d) $\alpha = 0.9$ and (e) $\alpha = 1.0$.

4.4. *Cell voltage behaviour*

When the operating current decreases with time in the manner $I(t) = \alpha I_L(t)$, the cell voltage also decreases. The cell voltage is described by Equation 18. Substituting Equations 23, 24 and 28 into Equation 18, the cell voltage as a function of time is given by

$$U(t) = U_0 + a_a + b_a \ln i + \Delta E + \frac{\alpha i_L(t)\Delta h}{\kappa_0} + \frac{RT}{zF}\ln(1-\alpha) + \Delta\phi_d \tag{30}$$

Figure 8 depicts the calculated values of the cell voltage against time for different values of α.

As indicated in Fig. 8 the cell voltage decreases steadily with time for all values of α, converging to

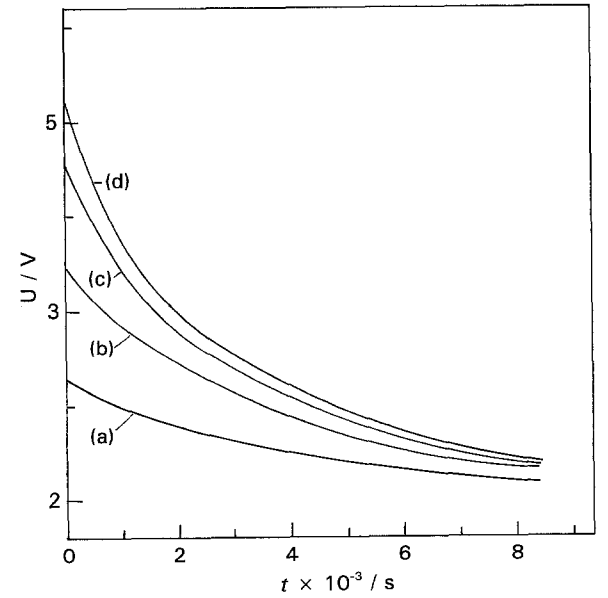

Fig. 8. Variation of cell voltage with time for pseudo potentiostatic conditions, for different values of α: (a) $\alpha = 0.25$, (b) $\alpha = 0.5$, (c) $\alpha = 0.75$ and (d) $\alpha = 0.9$.

a limiting value corresponding to the decomposition potential of water at infinite time.

5. Energy requirements

The total power requirement per unit of installed feeder area may be expressed as a sum of the electrical power and the power requirement for electrolyte pumping. In the case of a batch recirculating system the power requirement is time-dependent:

$$N(t) = U(t)i(t) + \frac{\alpha \Delta P u \Delta l}{L e_p} \tag{31}$$

The specific energy consumption (energy expended per unit product), may be expressed as

$$E = \int_0^{t_p} N(t)\,dt \Big/ \int_0^{t_p} r_e(t)\,dt \tag{32}$$

where r_e represents the electrochemical reaction rate for a desired product (in this case copper). The denominator in Equation 32 represents the quantity of reaction product per unit electrode area and for a given process time, t_p. Equation 32 may be integrated numerically for chosen limits. More explicitly, Equation 32 may be written in different forms depending on the mode of operation. Thus, for galvanostatic operation, the form of Equation 32 is

$$E = \frac{zF}{\frac{1}{t_p}\int_0^{t_p} e(t)\,dt}\left[\frac{1}{t_p}\int_0^{t_p} U(t)\,dt + \frac{\Delta PQ}{\alpha I_L(0) e_p}\right] \tag{33}$$

If the process occurs pseudopotentiostatically the specific energy consumption may be expressed as

$$E = \frac{zF}{e}\left[\frac{1}{t_p}\int_0^{t_p} U(t)\,dt + \frac{\Delta PQ}{e_p \frac{1}{t_p}\int_0^{t_p} I(t)\,dt}\right] \tag{34}$$

Equations 33 and 34 may be simplified by neglecting the pumping energy. It is known [17, 23] that this part of the energy requirement is much lower than that required for the electrochemical process. Equations 33 and 34 may be solved by numerical or graphical integration for the process time required to reach a specified amount of metal extraction. Figure 9 presents the relationships between the specific energy consumption and the quantity of extracted metal, obtained by graphical integration of Equation 33, for different values of α and for galvanostatic operation.

The specific energy consumption increases steeply when the degree of electrowinning reaches high values, for all values of α. From an energy point of view it is more attractive to carry out the process at lower values of α. However, this implies extension of the process time for a given degree of extraction, as depicted in Fig. 10, in which the process time is plotted against α for both galvanostatic (broken lines) and pseudopotentiostatic (full lines) modes of operation for various degrees of conversion. The differences in process times between the two modes for a given degree of conversion increase at lower values of α. Thus the galvanostatic mode is favoured from the standpoint of the process time needed to achieve a given degree of conversion.

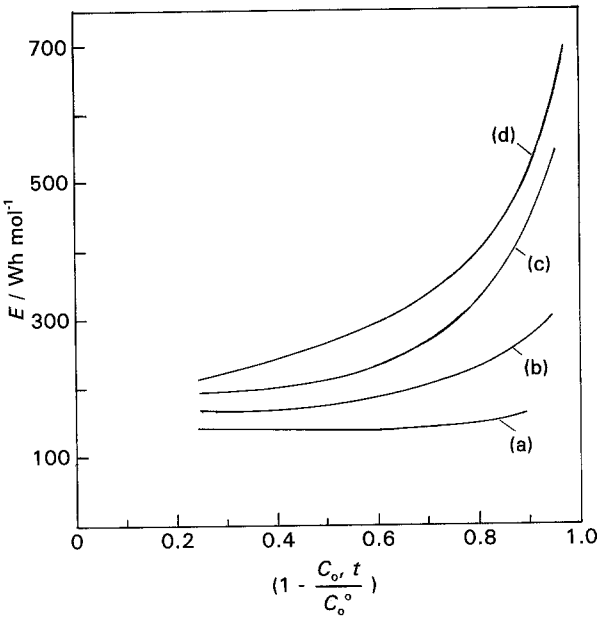

Fig. 9. Specific energy consumption against conversion degree at various α for galvanostatic conditions: (a) $\alpha = 0.25$, (b) $\alpha = 0.5$, (c) $\alpha = 0.75$ and (d) $\alpha = 0.9$.

The potentiostatic mode requires less energy as seen in Fig. 11, in which specific energy consumption is plotted against degree of conversion for different values of α. It is clear, comparing Figs 9 and 11 that the energy requirement per unit product is much lower for pseudopotentiostatic operation. For this mode energy consumption does not change markedly

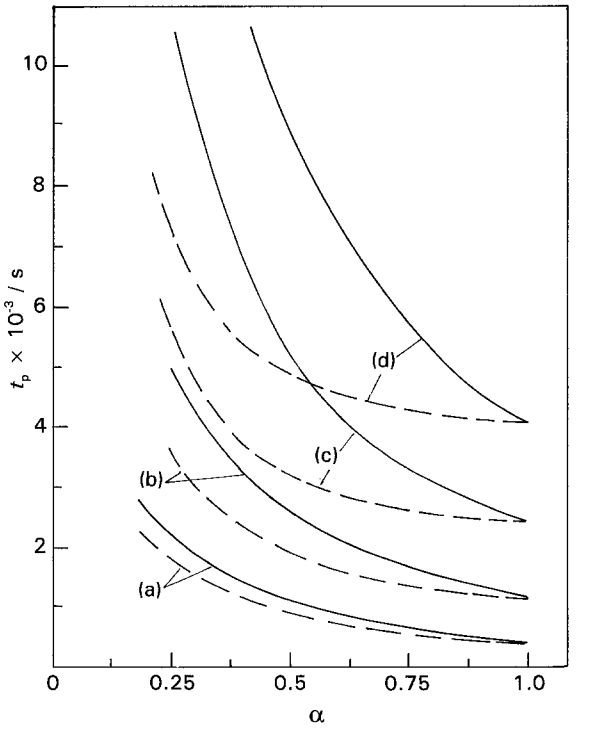

Fig. 10. Process time against α for various degree of conversion $1 - C_0(t)/C_0^0$: (a) 0.25, (b) 0.5, (c) 0.75 and (d) 0.95. (——) Pseudo potentiostatic conditions; (– – –) galvanostatic conditions.

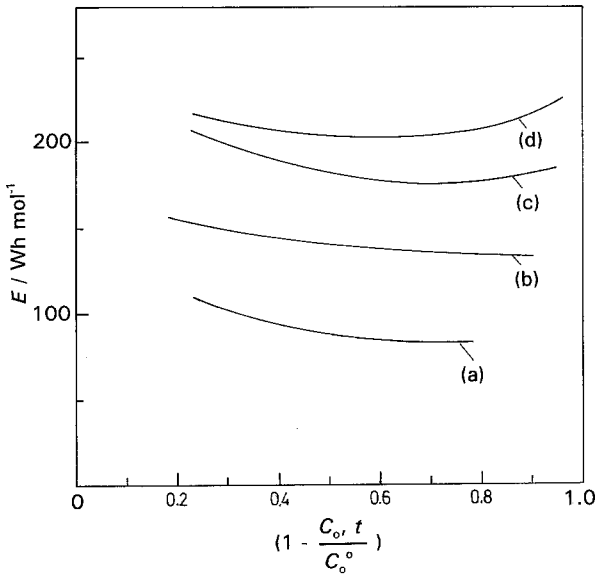

Fig. 11. Specific energy consumption against degree of conversion at various values of α: (a) $\alpha = 0.25$, (b) $\alpha = 0.5$, (c) $\alpha = 0.75$ and (d) $\alpha = 0.9$.

with degree of conversion whereas Fig. 9 shows very significant increases for the galvanostatic mode when the degree of conversion approaches one. The lower energy consumption with pseudopotentiostatic operation is a consequence of the avoidance of hydrogen evolution.

To elaborate on this point comparison of galvanostatic and pseudopotentiostatic modes from the standpoint of specific energy consumption and process time for the same degree of conversion is shown in Fig. 12. Clearly, the pseudopotentiostatic mode is the favoured option (full line) in regard to energy consumption. The process time is, however, shorter in galvanostatic mode (broken line). At higher α the difference in process times becomes smaller, indicating that the process should be carried out at high α and in pseudopotentiostatic

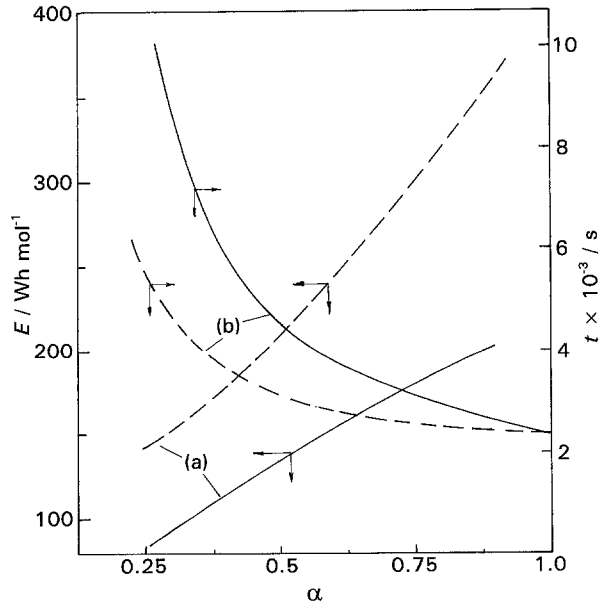

Fig. 12. Specific energy consumption and process time against α for the same degree of conversion: $1 - C_0(t)/C_0^0 = 0.5$. (——) Pseudo potentiostatic conditions; (– – –) galvanostatic conditions.

mode, making the process time shorter and taking advantage of the much reduced energy consumption. It is also clear from this figure that the process times are shorter for galvanostatic operation for the same degree of electrowinning.

6. Conclusions

In the modelling and analysis of galvanostatic and pseudopotentiostatic methods for copper electrowinning using three-dimensional electrode cells it may be concluded that:

(i) The present model allows an optimisation of the process which identifies the most favourable operating conditions.
(ii) The analysis has shown that the galvanostatic mode of operation ensures faster processing than the potentiostatic mode, for an equal initial current, resulting, after a certain time, in decreasing current efficiency and increasing specific energy consumption. With the potentiostatic method the current efficiency remains constant and the specific energy does not change significantly with the degree of extraction. Thus, the pseudopotentiostatic method of electrowinning is favourable in terms of energy saving and avoidance of hydrogen evolution, but the process time to reach a target degree of electrowinning is longer.

In the case of the pseudopotentiostatic mode of operation the challenge is the design of a suitable power supply and associated control system for an industrial cell which will ensure controlled decrease of the operating current with time, so as to follow the decay of the limiting current with time.

References

[1] M. Fleischmann, J. W. Oldfield and C. L. K. Tennakoon, *J. Appl. Electrochem.* **1** (1971) 103.
[2] J. A. E. Wilkinson and K. P. Haines, *Trans. Inst. Min. Met.* **81** (1972) C157.
[3] F. Coeuret, *Electrochim. Acta* **21** (1976) 185.
[4] G. Kreysa, *Chemie Ing. Techn.* **50** (1978) 332.
[5] D. Hutin and F. Coeuret, *J. Appl. Electrochem.* **7** (1977) 463.
[6] A. T. S. Walker and A. A. Wragg, *Electrochim. Acta* **25** (1980) 323.
[7] K. Scott, *J. Appl. Electrochem.* **18** (1988) 504.
[8] S. Germain and F. Goodridge, *Electrochim. Acta* **21** (1976) 545.
[9] V. D. Stankovic and S. Stankovic, *J. Appl. Electrochem.* **21** (1991) 124.
[10] V. D. Stankovic and A. A. Wragg, *ibid.* **14** (1984) 615.
[11] F. Goodridge and C. J. Vance, *Electrochim. Acta* **22** (1977) 1073.
[12] Cox and R. E. W. Jansson, *J. Appl. Electrochem.* **12** (1982) 205.
[13] D. Pletcher and J. T. Girault, Electrochemical Engineering, Loughborough, UK, *Inst. Chem. E Symp. series no. 98*, (1986) 15.
[14] Bennion and J. Newman, *J. Appl. Electrochem.* **2** (1972) 113.
[15] W. G. Sherwood, P. B. Queneau, C. Nikolic and D. R. Hodges, *Metal Trans.* **10B** (1979) 659.
[16] F. Coeuret and A. Storck, Éléments de Génie Électrochimique, Tec Doc, Paris (1984).
[17] L. H. Mustoe and A. A. Wragg, *J. Appl. Electrochem.* **13** (1983) 507.
[18] A. T. S. Walker and A. A. Wragg, *Electrochim. Acta* **22** (1977) 1129.

[19] A. P. K. Chu, M. Fleischmann and G. J. Hills, *J. Appl. Electrochem.* **4** (1974) 323.
[20] B. E. Bongenaar-Schlenter, L. J. J. Janssen, S. J. D. Van Stralen and E. Barendrecht, *J. Appl. Electrochem.* **15** (1985) 537.
[21] G. Kreysa and M. Kuhn, *ibid.* **15** (1985) 517.
[22] M. Enriquez-Granados, G. Valentin and A. Storck, *Electrochim. Acta* **28** (1983) 1407.
[23] V. D. Stankovic, 42st ISE Meeting Prague, 1990, Extended Abstracts vol. II, Paper 10/3.
[24] V. D. Stankovic, G. Lazarevic and A. A. Wragg, *J. Appl. Electrochem.*, in press.

Appendix: Estimation of hydrogen bubble effect on the effective conductivity of the electrolyte

The Bruggeman equation may be used to estimate the effect of hydrogen bubbles on the electrolyte conductivity. The consequent voltage drop term in Equation 20 (i.e., $\Delta\phi_H$) has the following form:

$$\frac{i_H(t)\Delta l}{\kappa_0(1-\epsilon_H)^{0.5}}$$

The maximum value of ϵ_H may be estimated as 0.13 for sulphuric acid electrolyte [21]. The above term may be calculated using $\Delta l = 0.01m$, $\kappa_0 = 50\,\Omega^{-1}\,m^{-1}$, $\epsilon_H = 0.13$ to give a value of $2.46 \times 10^{-4}\, i_H(t)$. The $i_H(t)$ value increases with decrease in $i_L(t)$, tending to reach the actual operating current when $i_L(t)$ reaches zero in accordance with Equation 6. It is thus possible to calculate the hydrogen bubble effect voltage loss term for any time after hydrogen evolution begins: the magnitude of the term never exceeds 45 mV which is less than 1.5% of the total cell voltage. Thus the omission of this 'difficult to calculate' term from Equation 20 is justified.

Strictly speaking, the value of ϵ_H of 0.13 cited above applies in free electrolyte flow at vertical plate electrodes. There is a need for information on gas bubble evolution and hold up in porous electrodes and the consequent effect on cell voltage demand. A further paper by the same group has recently investigated the effect of coevolution of hydrogen during copper deposition but mainly in relation to pressure drop effects [24].